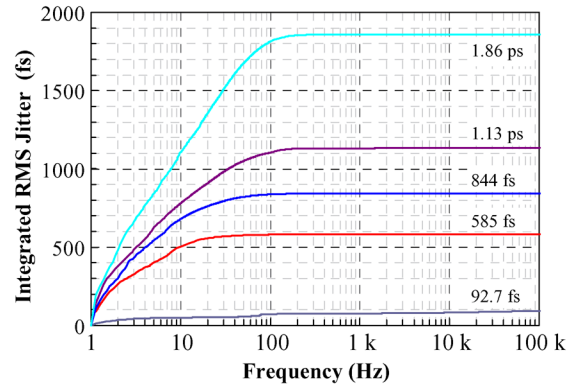
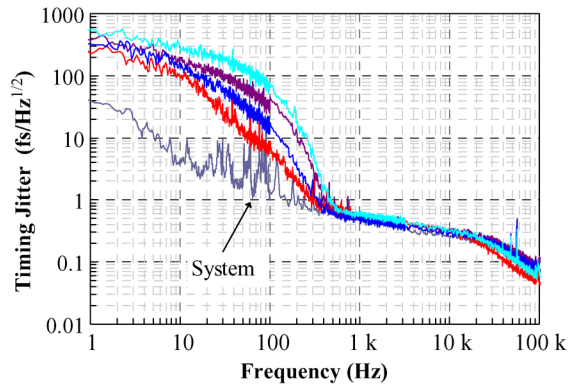


# Atmospheric Timing Transfer Using a Femtosecond Frequency Comb

Volume 2, Number 6, December 2010

Ravi P. Gollapalli, Student Member, IEEE  
Lingze Duan, Member, IEEE



DOI: 10.1109/JPHOT.2010.2080315  
1943-0655/\$26.00 ©2010 IEEE

# Atmospheric Timing Transfer Using a Femtosecond Frequency Comb

Ravi P. Gollapalli, *Student Member, IEEE*, and Lingze Duan, *Member, IEEE*

Department of Physics, The University of Alabama in Huntsville, Huntsville, AL 35899 USA

DOI: 10.1109/JPHOT.2010.2080315  
1943-0655/\$26.00 ©2010 IEEE

Manuscript received August 26, 2010; revised September 17, 2010; accepted September 18, 2010. Date of publication September 21, 2010; date of current version October 12, 2010. Corresponding author: L. Duan (e-mail: lingze.duan@uah.edu).

**Abstract:** We have experimentally demonstrated atmospheric transfer of microwave timing references using a femtosecond frequency comb. The excess timing jitter induced by the atmospheric propagation has been characterized, and evidence is provided to show that such characterization is not compromised by the parasitic effect of power-to-phase coupling in the photodetector. The fractional frequency stability for a 60-m total transmission distance is on the order of  $10^{-12}$  with a 1-s averaging time. The Allan deviation shows a  $\tau^{-1}$  dependence up to 500 s. Scale estimate confirms that the measured excess timing noise is caused by clear-air turbulence. Comparisons with previous works show that our results offer a more precise characterization of atmospheric timing transfer. The work may potentially help the development of high-fidelity synchronization for future free-space optical communications.

**Index Terms:** Timing, time dissemination, ultrafast optics, microwave photonics, phase noise, timing jitter.

## 1. Introduction

Free-space optical communication, with its enormous bandwidth capacity, will play a key role in the future free-space data networks, ranging from global-scale space-terrestrial links to local-scale metro-area networks [1]. As the bitrate is expected to continue its rapid climb to accommodate the ever-expanding data traffic, highly precise network synchronization will become imperative. This calls for a high-fidelity optical timing-distribution scheme. Over the last few years, there has been a growing interest in the study of laser-based remote transfer of timing references [2]–[6]. This is largely driven by the advance in atomic clocks and the advent of optical frequency combs, which conveniently bridge the frequency gaps between the microwave and the optical wavelength regions [7]. Much of the prior work, however, has been focused on timing transfer over fiber-optic links [2]–[4]. Recently, transfer of timing references through open atmospheric links has begun to draw research attentions. Notably, Sprenger *et al.* have studied the frequency stability for the transfer of both optical and radio frequency clock signals over a 100-m rooftop atmospheric link [5]. Djerroud *et al.* have demonstrated a 5-km coherent optical link by transmitting a narrow-linewidth laser beam through a turbulent atmosphere [6].

Generally, timing information can be optically transferred either at optical frequencies or at microwave frequencies [8]. The former requires the use of a highly stable single-frequency laser and aims to establish phase coherence of the optical carrier across the link. Such a scheme can usually achieve better fractional frequency stability compared with the latter case because of the much higher clock frequency (e.g., 100 THz versus gigahertz) [5], [6]. However, for applications in optical communication, due to the fact that the bits are coded on the optical carrier at microwave frequencies, this

scheme would require every user to be able to down-shift the clock frequency from the optical region to the microwave region, which adds substantial complexity to the user systems. On the other hand, timing transfer at microwave frequencies relies on the transmission of an amplitude modulated optical carrier with the modulator disciplined by an ultrastable microwave source such as an atomic clock. A key advantage of this scheme over the previous one is that it allows the users to conveniently recover the timing reference with direct photodetection [5].

Meanwhile, highly stable timing signals can also be distributed via direct transfer of a femto-second frequency comb (FFC) [8], which in essence is a femtosecond pulse train with well-stabilized repetition rates for both the envelope and the electric field [7]. Compared with the conventional carrier-modulation scheme, FFC-based timing transfer also allows for direct clock recovery using photodetectors but with better flexibility. This is because an FFC can simultaneously deliver a large number of frequency references as the harmonics of the pulse repetition rate  $f_R$ . The ultrashort pulsewidth allows the clock frequency  $f_C$  to be much greater than  $f_R$  (e.g., with a harmonic index  $f_C/f_R \gg 100$ ) and often only limited by the bandwidths of the photodetectors. Moreover, since one can use optical techniques (e.g., difference frequency generation) to lock an integer multiple of  $f_R$  directly to an optical frequency reference, such as an ultrastable laser [9], an FFC can potentially carry microwave clocks with ultralow phase noise because the clock uncertainty is only a small fraction of the frequency reference's uncertainty due to the frequency downshift.

FFC-based timing transfer has been shown to have comparable performance with the conventional carrier-modulation scheme in fiber-optic systems [8]. Given its aforementioned advantages, it would be interesting to see how this technique performs in free space. Here, we report what we believe to be the first experimental demonstration of FFC-based timing transfer across an open-atmosphere link. In Section 2, we will describe the experimental system, which will be followed by the measurement results in Section 3. Then, in Section 4, we will seek to validate our data by comparing them with known atmospheric parameters and results from previous works.

## 2. Experimental System

In order to study the atmospheric propagation of an FFC, we established an outdoor laser transmission link. The link is located on the roof of our laboratory building on the campus of The University of Alabama in Huntsville. The four-floor building has an observation platform about 20 m above the ground. There are no high-rise buildings or other tall structures nearby to render special wind patterns. A sturdy fixture is mounted on the platform to house a laser beam reflector (a 2-in gold mirror). The laser beam is launched from the control room via a fiber collimator and a couple of folding mirrors. The reflector sends the beam back to the control room, where all the signal processing and measurement takes place. The round-trip transmission distance is about 60 m.

The experimental setup for testing the microwave timing transfer is shown in Fig. 1. The system is divided into transmitting and receiving subsystems. In the transmitting part, a femtosecond fiber laser (Precision Photonics FFL-1560) generates a train of 120-fs pulses centered at 1560 nm, with a 90-MHz repetition rate and a 4-mW average power. An erbium-doped fiber amplifier (EDFA) boosts the power to about 100 mW while compressing the pulsewidth to below 100 fs. A 70:30 broadband fiber coupler directs the majority of this power into a fiber collimator, which launches a 7-mm-diameter beam into the atmospheric transmission link. A fiber-coupled variable attenuator is inserted before the collimator as a power regulator to provide precise control over the total optical power reaching the receiving photodiode.

In the receiving subsystem, the transmitted beam is tightly focused onto a high-speed photodiode, which recovers the repetition frequency of the femtosecond laser, as well as its harmonics. The tenth harmonic at 900 MHz is chosen as the microwave clock under test and is selected by a bandpass filter. To further reject the side modes, a local clock is used to beat the 900-MHz signal down to 35 MHz, where sharp low-pass filters can effectively remove all the remaining harmonics. Meanwhile, a reference clock signal is obtained by coupling a small portion of the EDFA output directly into the receiving subsystem via an optical fiber (the REF path in Fig. 1) and then using a microwave circuit similar to the transmitted clock. The resulting frequency signal serves two sets of

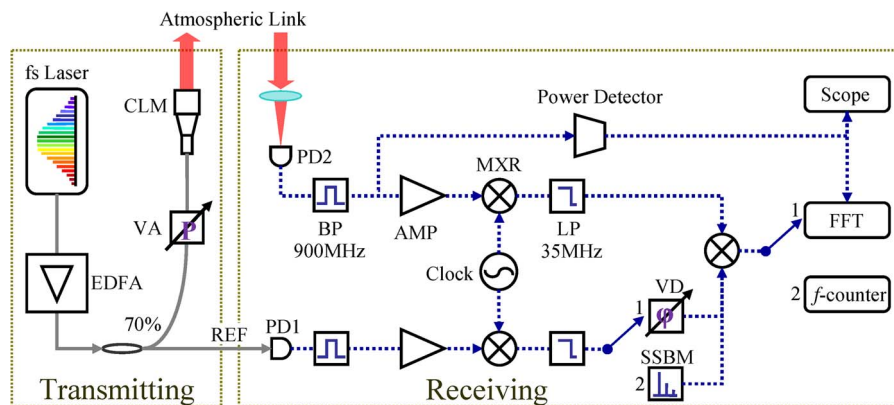


Fig. 1. Schematic layout of the test system for atmospheric microwave timing transfer. AMP: RF amplifiers; BP: bandpass filters; EDFA: erbium-doped fiber amplifier; LP: low-pass filters; MXR: double-balanced mixers; PD: photodiodes; VA: variable attenuator; VD: variable delay.

measurement. In the phase noise measurement, the reference clock passes through an adjustable delay line to gain a proper phase before it beats the transmitted clock in quadrature at a double-balanced mixer. The generated phase signal is frequency analyzed by a fast Fourier transform (FFT) analyzer (SRS SR785), and timing jitter spectral density is calculated from the phase noise spectrum. In frequency stability measurement, the reference clock is frequency shifted by 500 kHz through a single-sideband modulator (SSBM) and then mixed with the transmitted clock. This leads to a 500-kHz beat note, which is then measured with a frequency counter (SRS SR620) to determine its stability. It should be noted here that, although the repetition rate of the femtosecond laser is not stabilized in the test, the noise from the laser and the EDFA does not affect the measurement, because it is common mode in the above heterodyne scheme. This ensures correct characterization of the excess clock instability due to the atmospheric propagation.

### 3. Experimental Result

The measurement of the excess phase noise is conducted at different times of a day and under various weather conditions (except rainy days). The corresponding timing jitter is then calculated from the phase noise spectrum [8]. Fig. 2(a) shows several typical traces of the jitter spectral density, along with the system noise baseline. The excess timing jitter is above the baseline only at frequencies below several hundred hertz. The magnitude and frequency dependence of the jitter spectra are strongly affected by the weather conditions, particularly the wind speed, leading to a group of different spectral traces under otherwise similar conditions. The system baseline is mainly attributed to the radio frequency (RF) amplifiers in the receiving system, and the noise spikes around 10–200 Hz are believed to be due to electric interference caused by the utility circuitry in the control room. The scale of the excess timing jitter can be better evaluated by integrating the jitter spectral density over various frequency spans to obtain the root-mean-square (RMS) timing jitters. Fig. 2(b) shows the RMS jitter integrated from 1 Hz to the frequency in concern for all five traces in Fig. 2(a). Clearly, most contributions to the RMS jitter come from noise below 100 Hz, indicating the dominance of slow phase modulation. The total RMS jitters integrated from 1 Hz to 100 kHz range from several hundred femtoseconds to about 2 ps. The system noise proves to have a negligible effect in the measurement, as is evident from its sub-100-fs effective RMS jitter.

Two unique factors affecting the quality of atmospheric laser communication are beam wander and speckle [10]. Both effects have been visually observed in our experiment. One of their consequences is optical power fluctuation on the photodetector. When a photodiode is directly used to extract microwave clocks from an optical signal, such a power fluctuation can be converted into phase noise through power-to-phase coupling [11]. This detector-induced phase noise can make a significant contribution to the total measured phase noise. In order to minimize the power fluctuation

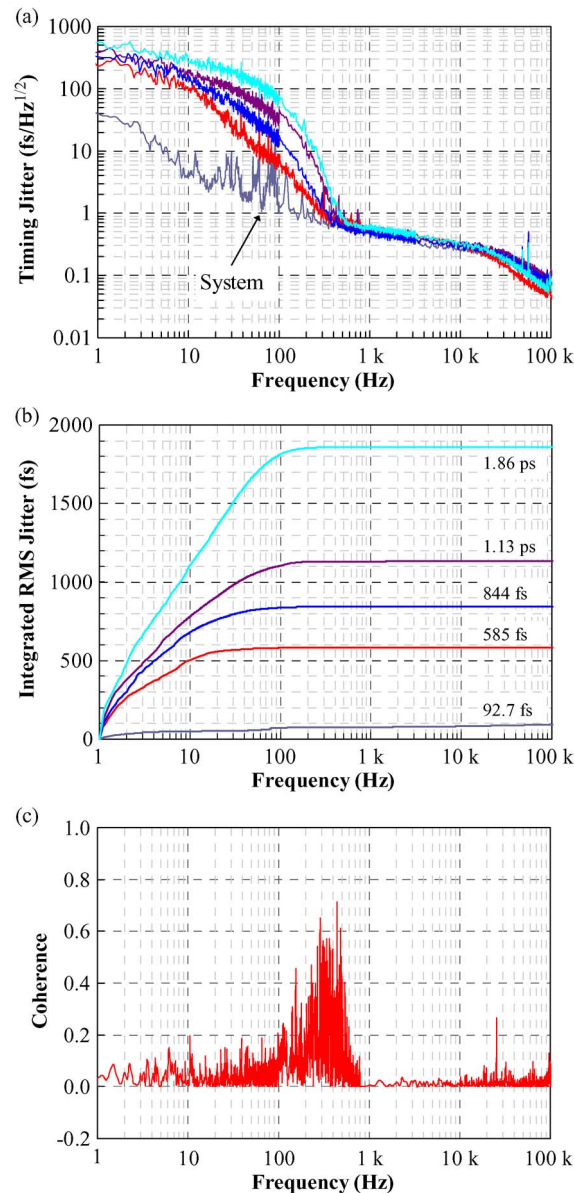


Fig. 2. (a) Some typical timing jitter spectral density along with the system noise. (b) Integrated RMS jitters for the five spectra in (a). The numbers are the RMS jitters integrated from 1 Hz to 100 kHz. (c) The near-zero coherence function between the clock phase and the clock power indicates that the measured excess noise is mainly due to the atmospheric propagation of the FFC.

and, hence, the impact of power-to-phase coupling, we use large-diameter optics (2-in diameter) in the receiving system and focus the beam directly onto the photodiode with the size of the focus relatively small compared with the active area of the detector. Such a configuration keeps the receiving system insensitive to the beam pointing drift and the transverse beam-profile fluctuation.

In the meantime, we monitor the power of the recovered 900-MHz clock with a microwave power detector (see Fig. 1) and evaluate the correlation between the phase noise and the clock power. This provides us with a means to validate the measured phase noise as primarily due to the atmospheric propagation. It has to be noted here that, under linear operation, the power of the recovered clock scales as the square of the optical power received by the photodiode. Around the average power,

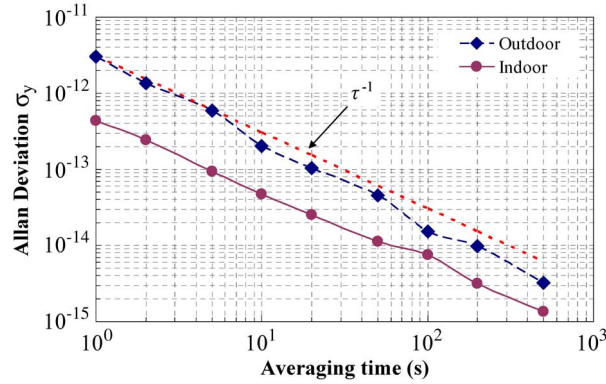


Fig. 3. Measured Allan deviation (diamond) shows an approximate  $\tau^{-1}$  dependence over the averaging time  $\tau$ . The baseline data (circle) are obtained under indoor conditions with a much lower wind speed.

however, the fluctuation of the clock power can be treated as linearly proportional to the fluctuation of the optical power. Therefore, the correlation between the phase noise and the fluctuation of the clock power actually reflects the correlation between the phase noise and the optical power fluctuation. The correlation is determined by recording the coherence function between the measured phase noise and clock power during each data run. Here, “coherence” is defined as

$$C_{yx}(f) = \frac{\Phi_{yx}(f)}{\sqrt{\Phi_{yy}(f) \cdot \Phi_{xx}(f)}} \quad (1)$$

where  $\Phi_{xx}(f)$  and  $\Phi_{yy}(f)$  are the power spectral densities of time series  $x$  and  $y$  (as functions of Fourier frequency  $f$ ), and  $\Phi_{yx}(f)$  is the cross-power spectral density between the two series.  $|C_{yx}(f)|^2$  can be directly measured with a dual-channel FFT analyzer (e.g., SR785). Fig. 2(c) shows the measured coherence function over a frequency range of 1 Hz to 100 kHz. Above 700 Hz, the phase noise and the clock power have little correlation. This is because the phase noise is below the system noise within this frequency range, as shown in Fig. 2(a). The system noise is mainly caused by the RF amplifiers used in the phase detection circuits and is totally independent from the power detection. The coherence is also close to zero from 1 Hz to 100 Hz, indicating that the measured phase noise has no correlation with the received optical power over a wide range of frequencies. Meanwhile, there is a moderate peak of coherence ( $\sim 0.5$ ) at a few hundred hertz, which is likely due to the scintillation of the laser beam causing temporal fluctuation of the irradiance [10]. However, the phase noise above 100 Hz rolls off quickly and provides very little contribution to the total RMS noise, as shown in Fig. 2(b). Therefore, the measured phase noise represents a fairly close account for the atmospheric transmission-induced phase noise.

The long-term timing transfer stability has been evaluated by measuring the Allan deviation of the 500-kHz beat note. The Allan deviation for a certain averaging time  $\tau$  is defined as

$$\sigma_y(\tau) = \left\langle \frac{1}{2} [\bar{y}(t+\tau) - \bar{y}(t)]^2 \right\rangle^{1/2} \quad (2)$$

where  $\langle \rangle$  represents an infinite time average, and  $\bar{y}$  denotes the average fractional frequency deviation relative to the nominal frequency over a period of  $\tau$  [12]. Fig. 3 shows a typical set of experimental data, along with a set of baseline data, which is obtained by transmitting the laser beam through a 10-m indoor transmission link with much lower airflow. The fractional frequency stability is on the order of a few parts per trillion with a 1-s averaging time. This is comparable with the frequency stability of most commercial atomic timing references, such as Cs and Rb clocks. At longer averaging times, the Allan deviation falls at a slope of  $\tau^{-1}$ , indicating white phase fluctuations [12]. This is different from fiber-optic transmission, where the Allan deviation falls at  $\tau^{-1/2}$  [2]. It should

also be noted that most atomic timing references display a  $\tau^{-1/2}$  behavior as well. As a result, transferring timing references through free space becomes more advantageous when the clock signal is averaged over longer time.

#### 4. Discussion

The propagation of an optical pulse train through an atmospheric communication channel is susceptible to the refractive-index fluctuation caused by clear-air turbulence [1], [13]. From the RMS timing jitter, we can derive the RMS fluctuation of the group index  $n_g$  by using the relation  $\Delta n_g = (c/L)\Delta T$ , where  $c$  is the speed of light in a vacuum,  $L$  is the total propagation distance, and  $\Delta T$  represents the RMS timing jitter of the FFC. By using  $\Delta T = 2$  ps and  $L = 60$  m, we find the value of  $\Delta n_g$  to be  $1 \times 10^{-5}$ . Meanwhile, it has been shown that  $\Delta n_g \approx a \cdot \Delta n$ , where  $\Delta n$  is the fluctuation of the phase index, and the proportional constant  $a$  is approximately equal to 3 in the visible and near-infrared wavelength range [14], [15]. This leads to an estimated RMS phase index fluctuation of several parts per million, which agrees with the well-known scale of such fluctuation due to clear-air turbulence [16].

The measured timing transfer stability is compared with a similar rooftop experiment over 100 m using the conventional carrier-modulation scheme [5]. The fractional instability at 1 s measured in our test is several times smaller than the result presented in [5]. Moreover, the Allan deviations reported in [5] appear to have an averaging-time dependence close to  $\tau^{-1/2}$  below 100 s, while our result is close to  $\tau^{-1}$ . Such a difference in the behavior of the Allan deviation indicates possible difference in the underlying mechanism of instability in these two experiments. In fact, as pointed out in [5], the earlier experiment is likely limited by the stability of the frequency synthesizers and, therefore, only offers the upper bound of the propagation-induced instability. This seems to be supported by the fact that the electronic timing instrument usually shows a  $\tau^{-1/2}$  characteristic. Such a system-noise limitation is partly caused by the low clock frequency (80 MHz) used in the earlier experiment [5]. In comparison, our experiment is free from such a restriction, as shown by the baseline data in Fig. 2(c), because the wide bandwidth of the femtosecond pulses allows the use of a higher harmonic of the repetition rate as the clock signal.

Further improvement of the transfer stability would require the use of active noise cancellation. Such a scheme has been demonstrated to be able to lower the transfer-induced instability by a factor of 10 in fiber-optic systems [17]. To apply a similar technique in free space, retroreflection is needed to allow the returning beam to travel exactly the same path back in order to avoid differences in phase noise caused by different paths. In addition, the locking system likely needs to have a much wider bandwidth compared with the fiber-optic scheme, even for a moderate transmission distance (e.g., 100 m) because of the fast refractive-index fluctuation due to turbulence.

In summary, we have experimentally demonstrated the transfer of microwave timing references over an open atmospheric link using an FFC. The excess timing jitter due to the atmospheric propagation is successfully characterized, and the result has been shown to suffer minimal impact from the parasitic power-to-phase coupling. The fractional frequency stability for a 60-m transmission is on the order of a few parts per  $10^{12}$  with a 1-s averaging time. The Allan deviation shows a  $\tau^{-1}$  dependence up to 500 s. These results agree well in scale with the clear-air turbulence model and offer a much more precise picture of the characteristics of atmospheric microwave timing transfer than previous works. Future work should focus on the mitigation of the propagation-induced excess clock instability by means of active noise cancellation.

---

#### References

- [1] V. W. S. Chan, "Free-space optical communications," *J. Lightw. Technol.*, vol. 24, no. 12, pp. 4750–4762, Dec. 2006.
- [2] K. W. Holman, D. J. Jones, D. D. Hudson, and J. Ye, "Precise frequency transfer through a fiber network by use of 1.5- $\mu\text{m}$  mode-locked sources," *Opt. Lett.*, vol. 29, no. 13, pp. 1554–1556, Jul. 2004.
- [3] N. R. Newbury, P. A. Williams, and W. C. Swann, "Coherent transfer of an optical carrier over 251 km," *Opt. Lett.*, vol. 32, no. 21, pp. 3056–3058, Nov. 2007.

- [4] G. Grosche, O. Terra, K. Predehl, R. Holzwarth, B. Lipphardt, F. Vogt, U. Sterr, and H. Schnatz, "Optical frequency transfer via 146 km fiber link with  $10^{-19}$  relative accuracy," *Opt. Lett.*, vol. 34, no. 15, pp. 2270–2272, Aug. 2009.
- [5] B. Sprenger, J. Zhang, Z. H. Lu, and L. J. Wang, "Atmospheric transfer of optical and radio frequency clock signals," *Opt. Lett.*, vol. 34, no. 7, pp. 965–967, Apr. 2009.
- [6] K. Djerroud, O. Acef, A. Clairon, P. Lemonde, C. N. Man, E. Samain, and P. Wolf, "Coherent optical link through the turbulent atmosphere," *Opt. Lett.*, vol. 35, no. 9, pp. 1479–1481, May 2010.
- [7] T. Udem, R. Holzwarth, and T. W. Hansch, "Optical frequency metrology," *Nature*, vol. 416, no. 6877, pp. 233–237, Mar. 2002.
- [8] S. M. Foreman, K. W. Holman, D. D. Hudson, D. J. Jones, and J. Ye, "Remote transfer of ultrastable frequency references via fiber networks," *Rev. Sci. Instrum.*, vol. 78, no. 2, p. 021101, Feb. 2007.
- [9] S. M. Foreman, A. Marian, J. Ye, E. A. Petrukhin, M. A. Gubin, O. D. Mücke, F. N. C. Wong, E. P. Ippen, and F. X. Kärtner, "Demonstration of aHeNe/CH<sub>4</sub>-based optical molecular clock," *Opt. Lett.*, vol. 30, no. 5, pp. 570–572, Mar. 2005.
- [10] L. C. Andrews and R. L. Phillips, *Laser Beam Propagation Through Random Media*, 2nd ed. Bellingham, WA: SPIE, 2005.
- [11] E. N. Ivanov, S. A. Diddams, and L. Hollberg, "Analysis of noise mechanisms limiting the frequency stability of microwave signals generated with a femtosecond laser," *IEEE J. Sel. Topics Quantum Electron.*, vol. 9, no. 4, pp. 1059–1065, Jul./Aug. 2003.
- [12] *IEEE Standard Definitions of Physical Quantities for Fundamental Frequency and Time Metrology*, IEEE Std. 1139-1988, 1983.
- [13] H. H. Su and M. A. Plonus, "Optical-pulse propagation in a turbulent medium," *J. Opt. Soc. Amer.*, vol. 61, no. 2, pp. 256–260, Feb. 1971.
- [14] P. E. Ciddor, "Refractive index of air: New equations for the visible and near infrared," *Appl. Opt.*, vol. 35, no. 9, pp. 1566–1573, Mar. 1996.
- [15] P. E. Ciddor and R. J. Hill, "Refractive index of air. 2. Group index," *Appl. Opt.*, vol. 38, no. 9, pp. 1663–1667, Mar. 1999.
- [16] K. S. Shaik, "Atmospheric Propagation Effects Relevant to Optical Communications," Jet Propulsion Lab., Cali. Inst. Technol., Pasadena, CA, TDA Progress Rep. 42–94, 1988.
- [17] K. W. Holman, D. D. Hudson, J. Ye, and D. J. Jones, "Remote transfer of a high-stability and ultralow-jitter timing signal," *Opt. Lett.*, vol. 30, no. 10, pp. 1225–1227, May 2005.